

Guiding Neutral Atoms on a Chip

N. H. Dekker,¹ C. S. Lee,^{1,2} V. Lorent,^{1,*} J. H. Thywissen,¹ S. P. Smith,¹ M. Drndić,^{1,2}
R. M. Westervelt,^{1,2} and M. Prentiss¹

¹*Department of Physics, Harvard University, Cambridge, Massachusetts 02138*

²*Division of Engineering and Applied Sciences, Harvard University, Cambridge, Massachusetts 02138*

(Received 16 August 1999)

We demonstrate the guiding of neutral atoms by the magnetic fields due to microfabricated current-carrying wires on a chip. Atoms are guided along a magnetic field minimum parallel to and above the current-carrying wires. Two guide configurations are demonstrated: one using two wires with an external magnetic field, and a second using four wires without an external field. These guide geometries can be extended to integrated atom optics circuits, including beam splitters.

PACS numbers: 32.60.+i, 03.75.-b, 05.60.Gg, 32.80.Pj

Recent decades have seen the development of the field of integrated optics, in which separate large-scale optical elements are replaced by miniaturized devices placed together on single chips. Devices such as modulators, polarizers, couplers, and splitters have been integrated on single substrates. This has permitted rapid development in technologies such as optical communication, since in addition to a considerable cost reduction, integration has led to an increase in reliability, reproducibility, and robustness [1].

Motivated by the possibility of similar advantages for atom optics, we have demonstrated two types of magnetic guides that can form building blocks for integrated atom optics. The atom guides demonstrated in this Letter are based on small, current-carrying wires deposited on substrates using photolithography [2]. A variety of guides for atoms, based on both optical [3] and magnetic interactions, have been proposed [4–7] and demonstrated [8–12]. The guides demonstrated in this paper are useful building blocks for integrated atom optics for the following reasons: (1) As the magnetic field is created by current-carrying wires, it can be dynamically reconfigured. (2) Because the wires are fabricated by photolithography, the features can be quite small (<150 nm), resulting in large magnetic field gradients and curvatures [13,14]. (3) Although the guides we demonstrate in this Letter support many transverse modes, existing fabrication can produce similar devices that support just one single mode [7]. (4) The atoms follow a magnetic field minimum located above the wires and are therefore easily accessible, making them compatible with atomic beam splitters in planar wire geometries. (5) The guides can link other planar atom optical elements [13] fabricated on the same substrate, forming robust, complex atom optical circuits. (6) Since the interactions are magnetic, all particles that have a permanent magnetic dipole moment can be manipulated.

If the atoms follow the magnetic fields adiabatically, the interaction potential between the atoms and the magnetic fields generated by the guide is given by $U = \mu_B g m |B|$, where μ_B is the Bohr magneton, g is the Landé factor, m is the magnetic quantum number, and B is the magnetic

field. Weak-field seeking atoms ($g_f m_f > 0$) feel a force towards the minimum of the magnetic field.

The two types of guides considered [7] are shown in Fig. 1. A two-wire guide is constructed using two wires with oppositely directed currents I and spaced by a distance S , as shown in Fig. 1(a). The direction along which the wires are spaced is indicated by \hat{x} , the direction perpendicular to the plane of the wires by \hat{y} , and the direction parallel to the length of the wires by \hat{z} . The field created by the current-carrying wires is proportional to a scaling field $B_0 = 2\mu_0 I / \pi S$ and is directed along $-\hat{y}$ between the two wires. To create a magnetic field minimum in a plane above the wires, a homogeneous external bias field

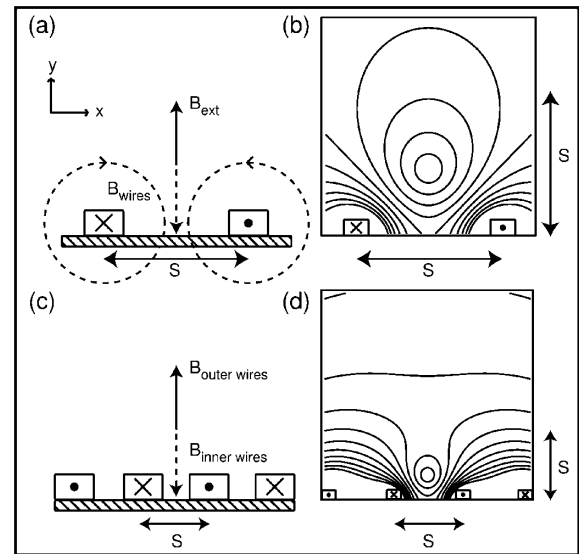


FIG. 1. (a) A two-wire magnetic guide: two gold wires spaced by S and with antiparallel current flow $\pm I$ are mounted on a sapphire substrate (cross-hatched). (b) For $B_{\text{ext}} = 10$ G and $B_0 = 20$ G, ten magnetic field contours spaced at $B_0/10$ are shown. (c) A four-wire magnetic guide: four gold wires are mounted on a sapphire substrate (cross-hatched). Adjacent wires spaced by S have oppositely directed currents. (d) For $B_{\text{inner}} = 20$ G and $B_{\text{outer}} = 13$ G, magnetic field contours of identical values as those in (b) are plotted.

$B_{\text{ext}}\hat{y}$ is applied to cancel the field due to the wires. The magnitude of the resulting total magnetic field is shown in the contour map of Fig. 1(b). Both the location of the magnetic field minimum and the resulting trap depth are determined by the competition between B_0 and B_{ext} . The location of the magnetic field minimum approaches the surface as B_{ext} is increased from zero until the minimum coincides with the surface at $B_{\text{ext}} = B_0$. It is desirable that the magnetic field minimum occur above the surface since atom-surface interactions can result in losses in guide transmission due to both adhesion and heating [15]. The maximum trap depth occurs at $B_{\text{ext}} = 0.5B_0$, for which the field minimum occurs at $y = S/2$. For a fixed ratio of B_{ext}/B_0 it is possible to vary the trap depth without altering the location of the magnetic field minimum. Typical parameters in our experiment are $S = 200 \mu\text{m}$ and $I = 0.5 \text{ A}$, yielding $B_0 = 20 \text{ G}$.

Figure 1(c) shows an alternate guide configuration that does not require an external bias field. A four-wire guide is constructed using four wires spaced by a distance S in which neighboring wires have oppositely directed currents. The inner pair produces a magnetic field proportional to a scaling field $B_{\text{inner}} = 2\mu_0 I_{\text{inner}}/\pi S$. However, instead of using an externally applied field to create a magnetic field minimum, the field of an outer pair of wires is used. This field scales as $B_{\text{outer}} = 2\mu_0 I_{\text{outer}}/3\pi S$. The magnitude of the resulting total magnetic field is shown in the contour map of Fig. 1(d). The location of the magnetic field minimum and the trap depth are now determined by the competition between B_{inner} and B_{outer} . Analogously to the two-wire guide, the location of the magnetic field minimum approaches the surface as B_{outer} is increased, with a minimum existing above the surface for $B_{\text{inner}}/9 < B_{\text{outer}} < B_{\text{inner}}$. Also similarly to the two-wire guide, for a fixed ratio of $B_{\text{outer}}/B_{\text{inner}}$ it is possible to vary the trap depth without altering the location of the magnetic field minimum. The maximum trap depth occurs at $B_{\text{outer}} = 0.7B_{\text{inner}}$, for which the field minimum occurs at $y \approx S/2$.

It is interesting to consider briefly the differences between two- and four-wire guides. The four-wire guide does not require an external field, which may be an advantage in integrating it with other atom optical components. In addition, for small two-wire atom guides ($S \sim 1 \mu\text{m}$), applying an appropriate B_{ext} may become difficult because the required field scales as I/S . The size of the confining potential in a four-wire guide, however, is significantly smaller than in a two-wire guide. This occurs because B_{outer} , which opposes B_{inner} , falls off with \hat{y} , in contrast to B_{ext} , which is uniform. One may observe this difference in trap size by comparing Figs. 1(b) and 1(d) [although note the scale change in Fig. 1(d) to accommodate four wires].

Fabrication of guide wires proceeds in two steps [2]: (1) mask-based photolithography followed by gold evaporation and lift-off, and (2) gold plating in solution to increase the cross-sectional area of the wires. Four parallel wires are made with a spacing of $200 \mu\text{m}$ and a wire length

of 1.2 cm . The wires are formed on a sapphire substrate, chosen for its high thermal conductivity and transparency. The wires terminate in 1 mm^2 contact pads that support indium seals into which contact wires are pressed. Each wire has an individual feedthrough connection. This permits simple switching between two- and four-wire guides without changing substrates.

The sapphire substrate is mounted on a copper cold finger that is cooled using liquid nitrogen to a temperature of 120 K . At this temperature, the resistance of the wires decreases, permitting higher currents to be run through the wires than at room temperature; however, at low currents ($\sim 150 \text{ mA}$) we operate the guide at room temperature. The substrate can be rotated in the \hat{x} - \hat{z} plane through an angle θ .

The experimental setup is shown in Fig. 2(a). Located approximately 1.5 cm in the \hat{z} direction above the sapphire substrate is a magneto-optical trap (MOT) containing 10^8 cesium atoms at a density of $5 \times 10^{10} \text{ atoms/cm}^3$. The atoms are dropped from the MOT and cooled to a temperature of approximately $15\text{--}20 \mu\text{K}$ by polarization gradient cooling. They are subsequently optically pumped to the weak-field seeking state $|F = 4, m_f = +4\rangle$ using a 1-mm-wide , σ^+ polarized optical pump beam tuned to both the $F = 3 \rightarrow F' = 4$ and $F = 4 \rightarrow F' = 4$ transitions, with a power of $1 \mu\text{W}$ in each component. We select these parameters to minimize heating of the atoms.

Atoms are detected below the guide by monitoring the absorption of a probe beam (waist $125 \mu\text{m}$) tuned to the

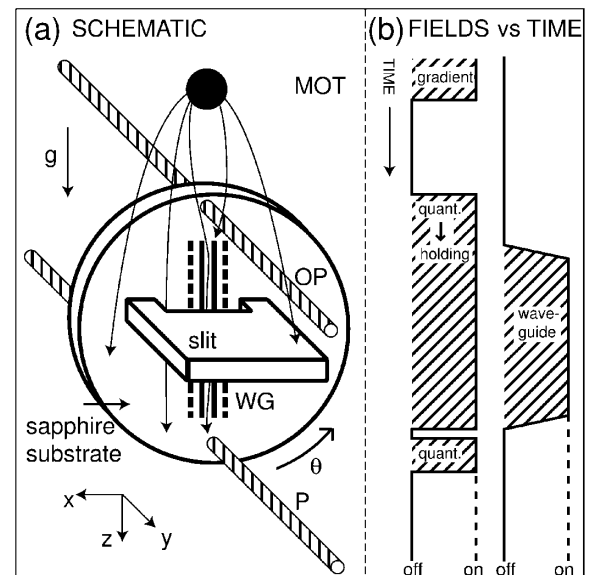


FIG. 2. (a) The experimental setup. Atoms released from the MOT fall under gravity. They pass through an optical pump beam (OP) and into the guide (WG). Atoms passing through a slit are detected by a probe beam P. (b) The magnetic fields as a function of time (see text). Care is taken to ensure all fields except a quantization field are off when the probe absorption is measured.

$F = 4 \rightarrow F' = 5$ transition. To avoid detection of atoms that do not interact with the guide, a stainless steel slit, which transmits only atoms close to the surface, is mounted approximately halfway down the length of the guide wires. The slit dimensions are 5.5 mm (\hat{x} direction) by 0.5 mm (\hat{y} direction). With the guide off, the small slit dimension in \hat{y} limits the range of the transverse velocity of the atoms detected below the slit to approximately the recoil velocity of Cs atoms.

The time sequence of the fields is shown in Fig. 2(b). All times are relative to an initial trigger pulse. Loading of the MOT is followed by the turn-off of the gradient field at 6 ms which leads to polarization gradient cooling until 17 ms. At 33 ms, a quantization field $B_q \hat{y}$ of magnitude 0.5 G is turned on and the atoms are optically pumped. The quantization field $B_q \hat{y}$ is rotated at 65 ms into a holding field $B_h \hat{z}$ of magnitude 0.25 G. The holding field ensures that the atoms adiabatically pass from the quantization field into the much larger field of the guide. At 66 ms, the guide fields are ramped on in approximately 2 ms. The guide fields and holding field are ramped down at 87 and 88 ms, respectively. A final quantization field $B_q \hat{y}$ of magnitude 0.5 G is applied at 90 ms for detection purposes.

In this experimental setup, the following spatial signatures of guiding are expected. The number of atoms detected below the guide output should increase with the guide operating because for a freely expanding MOT the density of atoms above the guide is higher than below it, and also because the gradient of the guide field will draw in additional atoms transversely displaced from the input of the guide. If the guide is positioned at an angle θ with respect to the \hat{z} direction defined by gravity, the position in \hat{x} of the maximum guide output signal should be spatially separated from the position in \hat{x} of the signal produced by atoms falling straight under gravity.

With the pulse sequence set up as described above, we scan the probe beam below the output of a two-wire guide in the \hat{x} direction to demonstrate these guiding effects. The result is shown in Fig. 3(a). The parameters used are $\theta = 9.4 \pm 0.5^\circ$, $I = 0.5$ A ($B_0 = 20$ G), and $B_{\text{ext}} = 10$ G. The absorption signal with guide current off (Δ) varies slowly as a function of probe position, with the peak signal at 0 mm. The absorption signal with the guide on (\bullet) can be more than an order of magnitude larger, indicating that atoms have been channeled into the guide. Furthermore, the guided peak is spatially distinct from the free flight peak and shows a maximum at approximately $x = +2.3$ mm.

The position scan clearly shows, in addition to a central feature at $x = +2.3$ mm, two side peaks at $x = +0.8$ mm and $x = +4.2$ mm. Such a spatial distribution agrees qualitatively with the results of classical numerical simulations, as shown in Fig. 3(b). The three features, from right to left, are due to (1) atoms that are deflected by the repulsive potential outside the guiding region, (2) atoms

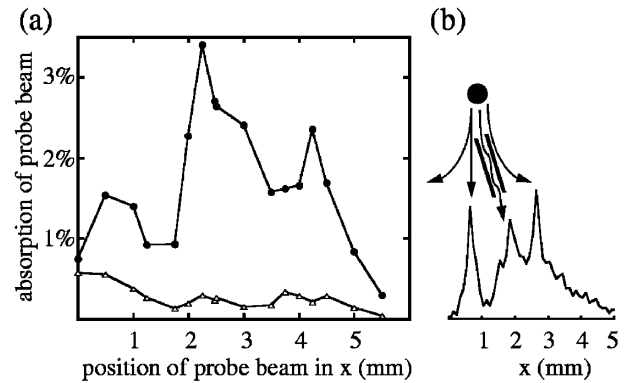


FIG. 3. (a) Absorption of probe beam versus position of probe in \hat{x} , taken with the guide off (Δ) and the guide on (\bullet) at a distance of 3.5 mm below the guide output. (b) Numerical simulation of the experiment, indicating, from right to left in \hat{x} , deflected atoms, guided atoms, and undeflected atoms.

that are guided by the confining potential, and (3) atoms that are undeflected because they crossed through the guide field at the unstable equilibrium point between the guiding and repelling potentials. Not observed in Fig. 3 are atoms that are deflected [as in case (1) above] towards $x < 0$ because the finite slit size in \hat{x} prevents transmission of these atoms.

In this experiment, several other signatures of guiding are observed: (1) We verify over a range of 20° that the location of the guide output follows the angle θ of the guide to within 10%. (2) No atoms are observed below the guide output when the circularity of the optical pump beam is reversed to pump the atoms into strong-field seeking states, as these atoms are repelled from the field minimum. (3) As the temperature of the atom source is increased, guiding efficiency decreases as fewer atoms are confined by the guiding potential.

Finally, we investigate the optimization of both two- and four-wire guides. As shown in Fig. 4, in a two-wire (four-wire) guiding configuration, we observe an optimum B_{ext} (B_{outer}) for a fixed B_0 (B_{inner}). In Fig. 4(a), at low values of B_{ext}/B_0 , both the trap depth and the magnetic field gradient are small, hence few atoms are guided. At higher values of B_{ext}/B_0 , the number of guided atoms increases

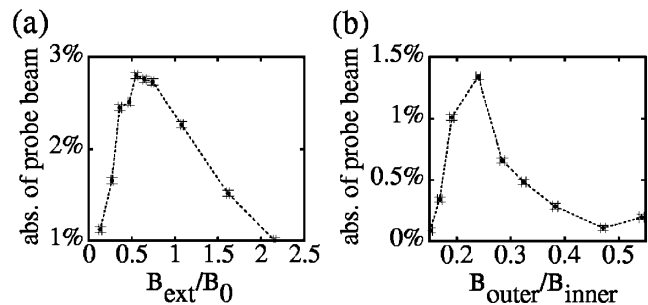


FIG. 4. (a) Absorption of probe beam below a two-wire guide as a function of B_{ext}/B_0 . (b) Absorption of probe beam below a four-wire guide as a function of $B_{\text{outer}}/B_{\text{inner}}$.

to a maximum at $B_{\text{ext}}/B_0 = 0.5 \pm 0.1$. This coincides well with the value of B_{ext} which optimizes the trap depth. We observe experimentally that the ratio of $B_{\text{ext}}/B_0 = 0.5$ which maximizes guiding is independent of the magnetic sublevel distribution of the atoms. As the value of B_{ext}/B_0 is increased further, the trap depth starts to decrease and the number of atoms guided correspondingly decreases. For $B_{\text{ext}}/B_0 > 1$, a magnetic field minimum no longer exists above the substrate. Nevertheless, the number of atoms detected is greater than if the guide were turned off: additional atoms pass through the slit as a result of the nonzero magnetic field gradient. This effect is dependent on the magnetic sublevel distribution of the atoms, as atoms in lower m_f states experience a weaker gradient for a given current than atoms in high m_f states. With an unpolarized source, additional atoms are observed out to $3.5B_{\text{ext}}/B_0$ rather than $2.1B_{\text{ext}}/B_0$.

Figure 4(b) shows a similar scan for a four-wire guide. The current in the inner wires is 0.15 A, yielding $B_{\text{inner}} = 6$ G. At low values of $B_{\text{outer}}/B_{\text{inner}}$, few atoms are guided as the inner wires dominate and no magnetic field minimum exists. As the value of $B_{\text{outer}}/B_{\text{inner}}$ increases beyond 0.15, however, a magnetic field minimum is created leading to an increase in the number of atoms guided. We find an optimum at approximately $B_{\text{outer}}/B_{\text{inner}} \approx 0.26$. Beyond this point, the number of atoms guided decreases as the magnetic field minimum gets pushed closer to the substrate surface and the trap size decreases. We observe that fewer atoms are guided in the four-wire guide than in the two-wire guide. We attribute this to the lower potential depths and smaller trap size in the four-wire guide. We further observe that the optimal guide configuration does not coincide with the maximum guide depth, possibly because the number of guided atoms also depends on the spatial extent of the guide.

Both two- and four-wire guides can have a finite number of transverse bound states and can therefore be single mode waveguides. Since the energy of the ground state scales inversely with the square of the guide diameter, the small size scale possible with microfabricated waveguides on a chip allows single mode operation with depths on the order of $10 \mu\text{K}$, orders of magnitude higher than previously demonstrated guides [3,7].

Atom beam splitters for interferometry are extensions of these chip-based guides. Consider a pair of two-wire guides that approach each other. When the distance between the pair is large compared to their wire spacing, two

separate guides exist. As the guides are brought together, the barrier between the potential wells can be controlled by the guide separation and the external field. At $1 \mu\text{m}$ length scales and for a fixed separation, the external field can control the tunneling between two single mode atom guides.

In conclusion, we have demonstrated the guiding of atoms with microfabricated wires on a chip. This work begins the development of atom guiding above surfaces to make integrated circuits for neutral atoms. The demonstrated guides represent key components of future integrated atom optics circuits [16].

We thank R. Younkin for comments and early work on this experiment, and M. Olshanii, M. Topinka, and G. Zabow for useful discussions. J.T. acknowledges support from the Fannie and John Hertz Foundation. This work was funded by ONR N00014-99-1-0347, NSF DMR-9809363, NSF PHY-9732449, and NSF PHY-9876929.

*Present address: Laboratoire de Physique des Lasers, Université Paris-Nord, F-93430 Villetaneuse, France.

- [1] T. Tamir, in *Guided Wave Optoelectronics*, edited by T. Tamir (Springer-Verlag, Berlin, 1988).
- [2] M. Drndić *et al.*, *Appl. Phys. Lett.* **72**, 2906 (1998).
- [3] J.P. Dowling and J. Gea-Banacloche, *Adv. At. Mol. Opt. Phys.* **37**, 1 (1996).
- [4] J.A. Richmond, S.N. Chormaic, B.P. Cantwell, and G.I. Opat, *Acta Phys. Slovaca* **48**, 481 (1998).
- [5] E.A. Hinds, M.G. Boshier, and I.G. Hughes, *Phys. Rev. Lett.* **80**, 645 (1998).
- [6] L.V. Hau, J.A. Golovchenko, and M.M. Burns, *Phys. Rev. Lett.* **74**, 3138 (1995).
- [7] J.H. Thywissen *et al.*, *Eur. Phys. J. D* **7**, 361 (1999).
- [8] J. Schmiedmayer, *Phys. Rev. A* **52**, R13 (1995); *Appl. Phys. B* **60**, 169 (1995).
- [9] J. Fortagh, A. Grossman, C. Zimmermann, and T.W. Hänsch, *Phys. Rev. Lett.* **81**, 5310 (1998).
- [10] J. Denschlag, D. Cassetari, and J. Schmiedmayer, *Phys. Rev. Lett.* **82**, 2014 (1999).
- [11] A. Goepfert *et al.*, *Appl. Phys. B* **69**, 217 (1999).
- [12] D. Müller *et al.*, *Phys. Rev. Lett.* **83**, 5194 (1999).
- [13] J.D. Weinstein and K.G. Libbrecht, *Phys. Rev. A* **52**, 4004 (1995).
- [14] We have fabricated $3\text{-}\mu\text{m}$ -wide wires carrying 10^8 A/cm^2 . For more details, see Ref. [2].
- [15] C. Henkel and M. Wilkens, *Europhys. Lett.* **47**, 414 (1999).
- [16] J. Schmiedmayer, *Eur. Phys. J. D* **4**, 57 (1998).